Ab Initio Molecular Orbital Calculations on $NO^+\cdot(H_2O)_n$ Cluster Ions. Part I: Minimum-Energy Structures and Possible Routes to Nitrous Acid Formation

Essam Hammam,[†,‡] E. P. F. Lee,[†,§] and J. M. Dyke*[,†]

Department of Chemistry, Southampton University, Southampton SO17 1BJ, U.K., Chemistry Department, Tanta University, Tanta, Egypt, and Department of Applied Biology and Chemical Technology, Hong Kong Polytechnic University, Hung Hom, Hong Kong

Received: December 6, 1999; In Final Form: February 16, 2000

Minimum energy geometries, harmonic vibrational frequencies, and stepwise binding energies have been obtained for the cluster ions $NO^+\cdot(H_2O)_n$, $n = 1-4$. From systematic ab initio calculations on the lighter $NO^+\cdot(H_2O)_n$ complexes ($n = 1-2$) at MP*n*, CCSD, and CCSD(T) levels of electron correlation with different basis sets, it was found that the MP2/6-311++G(2d,p) level of theory was reliable for the calculation of minimum-energy geometries and harmonic vibrational frequencies. Relative electronic energies were evaluated at the MP2/aug-cc-pVTZ//MP2/6-311++G(2d,p) level. The inclusion of zero point energy (ZPE) corrections, as well as counterpoise corrections for basis set superposition errors (BSSE), in the calculation of binding energies was essential to obtain the correct energy ordering for the different isomers of a cluster ion. The nature of the stepwise hydration processes was discussed based on the isomeric structures obtained. A reaction route for nitrous acid (HONO) formation when a water molecule is added to $NO^+\cdot(H_2O)_3$ has been established.

Introduction

A study of the hydration of NO^+ is of considerable interest not only because the information obtained would assist in the fundamental understanding of intermolecular hydrogen bonding[1,2] and ion solvation in this system, but also because it is important in understanding the role played by NO^+ in the chemistry of the upper atmosphere.[3] The main ions in the D region of the ionosphere below an altitude of ~82 km are water cluster ions of the form of $H^+\cdot(H_2O)_n$. Above ~82 km NO^+ is one of the principal ions and it is thought that solvated NO^+ converts via a series of reactions to $H^+\cdot(H_2O)_n$ below 82 km. It has been proposed by Ferguson and Fehsenfeld,[4,5] and independently by Good et al.,[6] that NO^+ undergoes a series of hydration steps with water to form $NO^+\cdot(H_2O)_n$ but, at a certain value of *n*, a bimolecular reaction with water to form a protonated water cluster and nitrous acid becomes thermodynamically favorable and dominates over formation of higher $NO^+(H_2O)_n$ clusters.

To study this mechanistic pathway, numerous laboratory gas-phase experiments have investigated the thermochemistry of the hydration process of NO^+. By using pulsed high-pressure ion source mass spectrometry, French et al.[7] derived values of 18.5 and 16.1 kcal/mol for the hydration enthalpies ($\Delta H_f°$, 298) of NO^+ and $NO^+\cdot(H_2O)$, respectively. From a vibrational predissociation laser spectroscopic study on $NO^+\cdot(H_2O)_n$ clusters with $n = 1-5$, Choi et al.[8] concluded that the NO^+ hydrates with $n = 1-3$ are ion−dipole complexes of H_2O ligands bound to the NO^+ core with all water molecules in the first solvation shell. The infrared spectra obtained are consistent with the fourth H_2O molecule binding, via a hydrogen bond, to the other water ligands, starting a second solvation shell. $NO^+(H_2O)_4$ exhibits two minor photodissociation channels not seen in the smaller clusters, loss of HONO and loss of two H_2O molecules, as well as the major channel which is loss of one water molecule. When $n = 5$, it was found that an $NO^+(H_2O)_5$ structure of the form of $H_3O^+(H_2O)_3$(HONO) explained the observed infrared spectrum as loss of HONO is the main loss channel. Recently, Stace et al.[9] showed using mass spectroscopy that the reaction $NO^+(D_2O)_n + D_2O \rightarrow (D_2O)_nD^+ + DONO$ becomes significant for $n = 3$ and is a dominant reaction path for $n = 4$ and beyond. In an attempt to remove the discrepancy over the level of hydration of NO^+ needed to promote the detection of proton hydrates, Angel and Stace[10] studied the collision-induced reactions of $NO^+(H_2O)_n$ cluster ions. From the analysis of the mass analyzed ion kinetic energy (MIKE) spectrum of $NO^+(H_2O)_n$ ($n = 3$, 4, 5), in which both unimolecular and collision-induced fragmentation were observed, Angel and Stace[10] suggested for $NO^+(H_2O)_3$ that neither collisional activation nor IR excitation[8] promotes loss of HONO, but that they both enhance the loss of water from the cluster ions as the major dissociation route. For $n = 3$, the results are consistent with all the ions being in the form $NO^+(H_2O)_3$. For $n = 4$, $NO^+(H_2O)_4$ is the major ion but a smaller number are in the form $H_3O^+(H_2O)_{n-2}$HONO. The latter structure becomes dominant for $NO^+(H_2O)_5$, where loss of HONO on collisional activation becomes greater than loss of H_2O. On the basis of the results of infrared spectra obtained for $NO^+(H_2O)_n$ with $n = 1-5$, Choi et al.[8] suggested that for $NO^+(H_2O)_3$ the three solvent ligands are in the first solvation shell and in $NO^+(H_2O)_4$ the fourth water molecule is hydrogen-bonded to two water molecules in the first solvation shell. For $n = 5$, the structure $H_3O^+(H_2O)_3$HONO was suggested, which would be consistent with the MIKE spectra recorded following collisional activation.[10] As a way of assisting the interpretation of the experimental findings, electronic structure calculations[8,11−13] have been undertaken on $NO^+(H_2O)_n$ clusters for $n = 1$, 2, 3. De Petris et al.[11] at the MP4(SDTQ)/6-311G**//MP2(FU)/6-31G**+ZPE(MP2(FU)/6-31G**) level of theory identified six different conformers for $NO^+(H_2O)$ with the nitrosohydro-

† Southampton University.
‡ Tanta University.
§ Hong Kong Polytechnic University.
* To whom correspondence should be addressed.

10.1021/jp994278t CCC: $19.00
Published on Web 04/20/2000

nium ion being the global minimum. The latter species is viewed as an ion−molecule complex between NO^+ and H_2O. Utilizing G1 theory, they obtained a heat of formation ($H_f°$, 298) of 160 ± 2 kcal/mol for that ion. Recently, using the Born−Oppenheimer molecular dynamics (BOMD) method within the framework of density functional theory (DFT) with a generalized gradient approximation (GGA), Ye and Cheng[13] studied $NO^+(H_2O)_n$ clusters up to the level of hydration of $n = 3$. For $n = 1$, they obtained a ground state in which NO^+ is connected, by a relatively weak bond, to the water molecule. They estimated the $NO^+\cdots H_2O$ bond to be 5% shorter than that calculated in previous MP2 studies.[8] When a second water molecule is added a new solvation shell is formed, in contrast to the proposition previously made by Choi et al.[8] using HF/6-31G** calculations. This second hydration shell gets completed upon the addition of a third water molecule. The binding energies are found to decrease as the hydration level increases and amount to 1.31, 0.87, and 0.77 eV for $n = 1$, 2, 3, respectively. A clear *drawback* of the DFT-GGA method is the overestimation of the electronic binding energy. The binding energy for $NO^+(H_2O)$, for example, is about 18%−30% or 5−8 kcal/mol larger than calculated by post-self-consistent field (SCF) molecular orbital methods.[8]

In a study on the protonated water clusters, $H^+(H_2O)_n$ with $n = 1-5$, at the MP2 level of theory, Lee and Dyke[14] demonstrated that the bonding in a cluster of this type is a balance between covalent and ion−dipole hydrogen bonding. As the hydration level n increases, dispersion effects become more important and can be treated by established electron-correlation methods. Recently, Paizs and Suhai[15] demonstrated in their study on the complexes $H_2O\cdot H_2O$, $H_2O\cdot HF$, $H_2O\cdot H_2S$, and $H_2S\cdot H_2S$ with DFT and MP2 levels of theory that, when dispersion forces become significant, DFT methods are inadequate to describe this type of interaction. Also in a study on $Ar\cdot NO^+$, Wright[16] concluded that DFT methods overemphasize the intermolecular bonding in an ionic complex of this type giving rise to short bond lengths and high harmonic vibrational frequencies. Considering all of these facts, the results of Ye and Cheng[13] obtained via a DFT method have to be taken with caution and the DFT methodology has not been employed in the present study.

At present, there is some level of agreement about the hydration level of NO^+ needed to promote the generation of proton hydrates and nitrous acid, but a clear description for the mechanism of nitrous acid formation is still lacking, either theoretically or experimentally. The aim of this contribution is to establish a reliable and economical theoretical approach for ab initio calculations on hydrated nitrosonium ion clusters, $NO^+(H_2O)_n$, with n up to 4. Clusters with $n > 2$ have not been considered by ab initio methods before. The global minimum for each cluster, its vibrational frequencies, and the route of nitrous acid HONO generation will all be investigated. A second paper which focuses on the thermodynamic parameters, $\Delta H°_{298}$, $\Delta S°_{298}$, and $\Delta G°_{298}$ for the stepwise hydration of $NO^+(H_2O)_n$ ($n = 1-4$), will be presented later.

Computational Details

The main aim of the calculations on the lighter clusters, $NO^+\cdot(H_2O)_n$, $n = 1$ and 2, is to establish a reliable methodology for calculations on the clusters with $n = 3$ and 4. In this connection, the effects of electron correlation and basis set size on the optimized geometries, harmonic vibrational frequencies, and relative energies were examined in a systematic way. Electron correlation effects on relative energies were studied by the MPn ($n = 2$, 3, and 4), CCSD, and CCSD(T) methods with the MP2/6-311++G(2d,2p) basis set, while the basis set size effects on the optimized geometries were examined by employing a variety of standard basis sets at the MP2 level. For geometry optimization and harmonic frequency calculations only the MP2 method was used, because of the availability of both analytic first and second derivatives at this level of theory. For clusters of the size considered in this work, the only practicable way for searches (and characterization) of stationary points on the energy hypersurface is with a correlation method which can calculate both the first and second energy derivatives analytically.

As will be discussed in the next section, it was found that for reliable minimum-energy geometries and harmonic vibrational frequencies, the MP2/6-311++G(2d,p) level is adequate. Therefore, for the heavier $NO^+\cdot(H_2O)_n$ clusters, where $n = 3$ and 4, geometry optimization and harmonic vibrational frequency calculations were only carried out at this level. However, for reliable relative energies, it was found that a larger basis set is required. It was decided that the MP2/aug-cc-pVTZ level was a reasonable compromise between reliability and economy. As a result, MP2/aug-cc-pVTZ energy calculations were carried out at the MP2/6-311++G(2d,p) minimum energy geometries for the heavier clusters, to obtain reliable relative energies.

The relative stability of various isomeric species can be derived by comparing their computed total electronic energies. However, because it is inevitable that limited basis sets have to be employed in practical ab initio calculations such as those performed in this work, it was valuable to also consider the interaction energy (ΔE_e) for the formation of a particular cluster by the solvation process:

$$NO^+\cdot(H_2O)_n + H_2O \rightarrow NO^+\cdot(H_2O)_{n+1} \qquad (1)$$

The full counterpoise (CP) correction for basis set superposition error (BSSE)[17] was employed in the evaluation of interaction energies (ΔE_e) for the stepwise hydration processes. However, for the formation of $HONO\cdot(H_3O)^+\cdot(H_2O)_2$, given by

$$NO^+\cdot(H_2O)_3 + H_2O \rightarrow HONO\cdot(H_3O)^+\cdot(H_2O)_2 \qquad (2)$$

the CP correction was not carried out, because the product complex has a very different structure from that of the reactants. Equation 2 does not represent a complex formation process as denoted by eq 1 but is a chemical reaction, involving bond breaking and formation. Nevertheless, at the MP2/aug-cc-pVTZ level, the calculated total BSSE was found to be relatively small (<1.0 kcal/mol; see next section) for most of the complex formations considered here. It seems reasonable therefore, to assume that, for formation of $HONO\cdot(H_3O)^+\cdot(H_2O)_2$, the BSSE involved in the evaluation of the reaction energy of reaction 2 would not be more than 1 kcal/mol.

All calculations were carried out using the GAUSSIAN 94 suite of programs.[18]

Results and Discussion

The geometry optimizations and harmonic frequency calculations performed in this work have two main aims. The first is to locate the global minima of the various $NO^+\cdot(H_2O)_n$ clusters, for $n = 1-4$. The second is to locate possible reaction routes for formation of nitrous acid in the hydration process of the NO^+ cation. Before the results of the geometry searches are presented the reliability of the different levels of theory employed in the calculations on the smaller clusters ($n = 1$ and

TABLE 1

(a) Geometry and Electronic Energy of the Optimized C_s-Constrained Structure of $NO^+ \cdot H_2O$ Cluster at Different Levels of Theory

method	$r(O_1-N_2)$/Å	$r(N_2-O_3)$/Å	$r(H_4-O_1)$/Å	$\theta(O_1-N_2-O_3)$/°	$\theta(H_4-O_1-N_2)$/°	δ/°	$-E_e$/Hartree
HF/6-31G(d)	2.3247	1.0429	0.9524	100.2	125.7	15.3	204.956450
MP2/6-31++G(d,p)	2.2959	1.1064	0.9692	98.0	123.1	26.0	205.516011
MP2/aug-cc-pVDZ	2.2819	1.0999	0.9710	98.4	121.7	31.3	205.579990
MP2/6-311G(d,p)	2.2549	1.0897	0.9634	98.6	122.3	30.0	205.607368
MP2/6-311++G(d,p)	2.3309	1.0887	0.9649	96.5	124.5	23.3	205.617671
MP2/6-311++G(2d,p)[a]	2.2976	1.0868	0.9685	98.1	123.1	26.7	205.654178
CCSD(T)/6-311++G(2d,p)[b]	2.2976	1.0736	0.9682	98.9	123.5	25.3	205.676617
MP2/6-311++G(3df,2pd)	2.2927	1.0829	0.9639	97.5	123.1	27.2	205.725632

(b) Calculated Counterpoise-Corrected Electronic Interaction Energy ΔE_e(cp) Total Basis Set Superposition Error $BSSE_{total}$ and Zero Point Energy Difference ΔZPE[c] in kcal·mol^{-1} for the reaction $NO^+ + H_2O \rightarrow NO^+ \cdot H_2O$

method	$BSSE_{total}$	ΔE_e(cp)	ΔE_e(cp) + ΔZPE
MP2/6-311++G(d,p)	1.76	−19.69	−17.92
MP2/6-311++G(2d,p)	1.38	−19.96	−18.19
MP2/6-311++G(2d,2p)[c]	0.87	−19.44	−17.67
MP2/6-311++G(3df,2pd)	0.61	−19.93	−18.16
MP2/aug-cc-pVTZ[c]	0.51	−20.29	−18.52
MP2/aug-cc-pVQZ[c]	0.22	−20.59	−18.82
MP3/6-311++G(2d,2p)[c]	0.84	−18.86	−17.09
MP4D/6-311++G(2d,2p)[c]	0.85	−18.89	−17.12
MP4DQ/6-311++G(2d,2p)[c]	0.82	−18.52	−16.75
MP4SDQ/6-311++G(2d,2p)[c]	0.79	−18.88	−17.11
CCSD/6-311++G(2d,2p)[c]	0.83	−18.68	−16.91
CCSD(T)/6-311++G(2d,2p)[c]	0.92	−19.24	−17.47

[a] The calculated harmonic vibrational frequencies in cm^{-1} (IR intensities in km·mol^{-1}) are: a′: 213(2), 242(73), 400(272), 1645(71), 2110(43), 3766(143); a″: 97(15), 421(76), 3872(178). [b] It can be seen that the geometrical parameters obtained at this level are similiar to those at the MP2 level using the same basis set. [c] Calculated at the MP2/6-311++G(2d,p) optimized geometry.

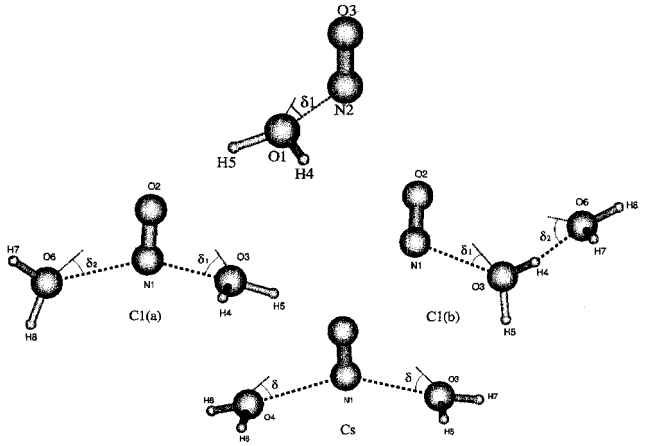

Figure 1. The optimum structures for the isomers of $NO^+ \cdot (H_2O)_{n=1,2}$ clusters predicted at MP2/6-311++G(2d,p) level of theory.

2) are first discussed. This provides the foundation for the more computationally demanding calculations on the larger clusters.

$NO^+ \cdot H_2O$. The computed parameters for the optimized geometry (Figure 1), relative energies (interaction energy with the counterpoise correction for BSSE), and the harmonic frequencies obtained at various levels of calculation are summarized in Tables 1a and 1b, respectively. The minimum-energy structure has a C_S symmetry in agreement with those previously reported in the literature[8,13] although some geometrical parameters differ significantly (Table 1a). Because previously reported calculations are at rather low levels of theory (MP2/6-31G* and DFT), the results obtained here should be more reliable. When the MP2/6-311++G(2d,p) and MP2/6-311++G(3df,2pd) optimized geometrical parameters shown in Table 1a are compared, it is very pleasing to see that the differences in the geometrical parameters obtained at the two levels of calculation are very small (<0.005 Å and 0.6°, for the intermolecular bond length and angle respectively). It can be concluded that the basis set effects have been essentially exhausted, and the MP2/6-311++G(2d,p) level is adequate for reliable calculation of geometrical parameters. The CCSD(T)/6-311++G(2d,p) optimized geometrical parameters are also in agreement with these values.

For the harmonic frequencies (Table 1a), the highest level of calculation which could be carried out with the available computational resources was at the MP2/6-311++G(2d,p) level. The harmonic frequencies obtained with smaller basis sets are probably less reliable. In view of the very similar optimized geometries obtained at the MP2/6-311++G(3df,2pd) and MP2/6-311++G(2d,p) levels, it is believed that the harmonic frequencies obtained with the 6-311++G(2d,p) basis set are reliable, and should be adequate for the purpose of zero-point-energy (ZPE) correction.

Considering relative energies (Table 1b), the oscillation in the results obtained with the MPn (n = 2, 3, and 4) methods is as expected and can be considered to be small (<0.5 kcal/mol). The contribution of triple excitations to the CCSD binding energy is significant, but not considerable (ca. 0.5 kcal/mol). It seems that the level of electron correlation is not as important as the basis set size in the evaluation of relative energies for this kind of system. For the same basis set (6-311++G(2d,p)), the MP2 method gives an interaction energy of −19.44 kcal/mol (CP corrected, without ZPE correction; Table 1b), which differs from that of the CCSD(T) method (−19.24 kcal/mol) by only 0.20 kcal/mol (Table 1b). This suggests that the MP2 method is probably adequate for binding energies in this kind of cationic complex (although there is almost certainly cancellation of errors in the derivation of the binding energy). Regarding the basis size, the aug-cc-pVQZ basis set, which is the largest basis set used, should give the most reliable interaction energy. The very small $BSSE_{total}$ of 0.22 kcal/mol obtained with this basis suggests that it is very close to basis saturation. However, use of the aug-cc-pVQZ basis set was found to be too time-consuming for calculations on the larger clusters (n = 3, 4). The combination of the MP2 method with

TABLE 2: Geometries, Electronic Energies, and Standard Entropies for C_s and C_1 Optimized Structures of $NO^+\cdot(H_2O)_2$ Cluster at MP2/6-311++G(2d,p) Level of Theory; Bond Lengths Are Given in Å, Angles in Degrees

C_s[a,b]		C_1(a)[a]		C_1(b)[a]	
$r(N_1-O_2)$	1.0859	$r(N_1-O_2)$	1.0867	$r(N_1-O_2)$	1.0948
$r(N_1-O_3)$	2.4050	$r(N_1-O_3)$	2.3552	$r(N_1-O_3)$	2.0914
$\theta(O_2-N_1-O_3)$	93.9	$r(N_1-O_6)$	2.3639	$r(H_4-O_6)$	1.6505
$\theta(O_3-N_1-O_4)$	118.7	$\theta(O_2-N_1-O_3)$	95.7	$\theta(O_2-N_1-O_3)$	104.1
$\omega(O_2-N_1-O_3-H_5)$	101.7	$\theta(O_2-N_1-O_6)$	103.1	$\theta(H_4-O_6-H_7)$	119.5
$\omega(O_2-N_1-O_3-H_7)$	−109.3	$\theta(O_3-N_1-O_6)$	95.7	$\omega(O_2-N_1-O_3-H_4)$	73.5
δ	21.0	$\omega(O_2-N_1-O_6-H_7)$	1.7	$\omega(O_3-H_4-O_6-H_7)$	−87.5
		$\omega(O_2-N_1-O_6-H_4)$	111.0	δ_1	42.4
		δ_1	24.0	δ_2	28.3
		δ_2	13.0		
E_e/Hartree	−281.972364	E_e/Hartree	−281.9723986	E_e/Hartree	−281.9710806
$S°$/cal·mol^{-1}·K^{-1}	92.2	$S°$/cal·mol^{-1}·K^{-1}	92.1	$S°$/cal·mol^{-1}·K^{-1}	86.9

[a] See Figure 1. [b] The calculated harmonic vibrational frequencies in cm^{-1} (IR intensities in km·mol^{-1}) are: a′: 28(0), 90(10),163(5), 214(21), 375(496), 393(127), 1652(67), 2117(15), 3788(54), 3893(240); a″: 40(3), 187(0), 217(15), 356(103), 360(41), 1649(100), 3786(129), 3892(67).

the aug-cc-pVTZ basis set seems to be a reasonable compromise between reliability and economy. The BSSE of 0.51 kcal/mol at the MP2/aug-cc-pVTZ level is acceptable, as compared with a normally accepted chemical accuracy of ±1 kcal/mol.

Very recently an ab initio study on some hydrogen-bonded complexes has appeared.[19] This work investigated the effects of basis set and treatment of electron correlation on the computed interaction energy for the formation of $H_2O\cdot MeOH$, $H_2O\cdot MeO$, $H_2O\cdot H_2CO$, $MeOH\cdot MeOH$, and $HCOOH\cdot HCOOH$ complexes. The conclusions of this work were very similar to those reached above—that the MP2 method gives results which are similar to those of the CCSD(T) method, and a large basis set is required to obtain a reliable interaction energy.

$NO^+\cdot(H_2O)_2$. Three structures of the dihydrate were considered (Figure 1) and they were all found to be true minima (with all real frequencies). Two of these structures, C_s and C_1(a) have the two water molecules both bonded to N in the first solvation shell, while the third structure C_1(b) has the second water molecule hydrogen-bonded to the first water molecule in the second solvation shell. The results are summarized in Tables 2 and 3.

As was the case for the monohydrate discussed above, only the results of the present work are presented because previous calculations were at lower levels. The general trends of the results for the dihydrate with the levels of calculation are very similar to those observed and discussed above for the monohydrate. This is so for all three structures of the dihydrate considered, and the comparison of results with different basis set and level of electron calculation will not be repeated. It is clear that the conclusions reached for the monohydrate on the basis set size effects and the levels of correlation hold also for the dihydrate. Hence, it seems reasonable to assume that they would hold also for the larger clusters considered in this study. In summary, the MP2/6-311++G(2d,p) level of calculation is expected to be adequate for obtaining reliable geometries and harmonic vibrational frequencies for the larger clusters, and the MP2/aug-cc-pVTZ//MP2/6-311++G(2d,p) level of calculation should be able to derive reliable relative energies.

Considering the computed total electronic energies, structure C_1(a) has the lowest energy, which is only very slightly lower than structure C_s (by ca. 0.02 kcal/mol; Table 3). However, after correcting for BSSE and ZPE, the relative energy ordering changes and the C_s structure becomes the lowest energy isomer, but only by less than 0.1 kcal/mol (Table 3). The slightly larger BSSE (by ca. 0.04 kcal/mol) for structure C_1(a), which is probably due to its slightly shorter intermolecular bond lengths (2.3552 and 2.3639 Å; Table 2) as compared with that of structure C_s (2.4050 Å), is a factor which contributes to the change of the energy ordering, whereas the ZPE difference (ca. 0.1 kcal/mol) is the other factor. Clearly, both isomeric structures are very close in energy and both would be present under normal experimental conditions at room-temperature. For the sake of simplicity, however, the C_s structure will be considered in the following as the global minimum of the dihydrate.

Structure C_1(b) has the second water molecule in the second solvation shell and it is ca. 1 kcal/mol higher in energy than the global minimum. Note that the BSSE for the second water is significantly larger (by ca. 0.5 kcal/mol, depending on the level of calculation), when compared with that in the structures C_S and C_1(a). This is probably because of the shorter intermolecular bond length between the two water molecules (O···H hydrogen-bond length of 1.6505 Å; Table 2) in the structure C_1(b) as compared to the longer N···O intermolecular bond lengths in the other two structures. These considerations show the rather demanding requirements on the level of calculation, particularly on the quality of the basis set, in the study of the relative stability of this type of cluster. Nevertheless, at the MP2/aug-cc-pVTZ//MP2/6-311++G(2d,p) level, the $BSSE_{total}$ of 0.7 kcal/mol for the C_1(b) structure would still be considered as acceptable. A discussion of the various interactions in the different isomeric structures of the whole series of the clusters considered in this work will be given later.

Having performed calculations on $NO^+\cdot(H_2O)$ and $NO^+\cdot(H_2O)_2$ with different basis sets and levels of electron correlation as explained above, it was decided, on the basis of the results obtained, to optimize the geometries of $NO^+\cdot(H_2O)_3$ and $NO^+\cdot(H_2O)_4$ at the MP2/6-311++G(2d,p) level and calculate relative energies at the MP2/aug-cc-pVTZ level.

$NO^+\cdot(H_2O)_3$. Seven structures of the trihydrate were optimized at the MP2/6-311++G(2d,p) level (Figure 2 and Table 4a). These structures have water molecules in one (C_S(a) and C_{3v}), two (C_S(b), C_S(c), C_1(a), and C_1(c)) and three (C_1(b)) solvation shells, respectively. Five structures were found to be minima, and two were found to be saddle points (Table 4b). For the saddle point structures, C_{3v} and C_S(c), when their respective symmetry constraints were relaxed (according to the normal mode with an imaginary frequency), they optimized to the structures C_S(a) and C_1(c), respectively. The results are summarized in Table 4. Note that in calculating the interaction energies for the stepwise complex formation of the various trihydrate isomeric structures (Table 4c), different dihydrate isomeric structures were considered for the corresponding trihydrate structure formation, because only a certain dihydrate structure could lead to a corresponding trihydrate structure by the addition of a free water molecule at an appropriate site. Hence, the computed interaction energies correspond to indi-

TABLE 3

(a) Calculated Counterpoise-Corrected Electronic Interaction Energy ΔE_e(cp), Total Basis Set Superposition Error $BSSE_{total}$, and zero Point Energy Difference ΔZPE^a in kcal·mol^{-1} for the cluster $NO^+\cdot(H_2O)_2$ of C_s Symmetry, (See Figure 1)

method	BSSE($NO^+\cdot H_2O$)	BSSE(H_2O)	$BSSE_{total}$	ΔE_e(cp)	ΔE_e(cp) + ΔZPE
MP2/6-311++G(2d,p)	0.36	1.06	1.42	−16.21	−14.73
MP2/6-311++G(2d,2p)[a]	0.38	0.54	0.92	−15.81	−14.33
MP2/6-311++G(3df,3pd)[a]	0.33	0.33	0.66	−16.14	−14.66
MP2/aug-cc-pVTZ[a]	0.28	0.18	0.46	−16.13	−14.65
MP2/aug-cc-pVQZ[a]	0.13	0.08	0.21	−16.36	−14.88
MP3/6-311++G(2d,2p)[a]	0.40	0.49	0.89	−15.77	−14.29
MP4D/6-311++G(2d,2p)[a]	0.39	0.50	0.89	−15.68	−14.20
MP4DQ/6-311++G(2d,2p)[a]	0.38	0.48	0.86	−15.61	−14.13
MP4SDQ/6-311++G(2d,2p)[a]	0.38	0.51	0.89	−15.60	−14.12
CCSD/6-311++G(2d,2p)[a]	0.38	0.50	0.88	−15.58	−14.10
CCSD(T)/6-311++G(2d,2p)[a]	0.41	0.57	0.98	−15.67	−14.19

(b) Calculated Counterpoise-Corrected Electronic Interaction Energy ΔE_e(cp), Total Basis Set Superposition Error $BSSE_{total}$ and Zero Point Energy Difference ΔZPE^a in kcal·mol^{-1} for the Cluster $NO^+\cdot(H_2O)_2$ of C_1(a) Symmetry (See Figure 1)

method	BSSE($NO^+\cdot H_2O$)	BSSE(H_2O)	$BSSE_{total}$	ΔE_e(cp)	ΔE_e(cp) + ΔZPE
MP2/6-311++G(2d,p)	0.41	1.04	1.45	−16.20	−14.62
MP2/6-311++G(2d,2p)[a]	0.45	0.51	0.96	−15.79	−14.21
MP2/aug-cc-pVTZ[a]	0.33	0.20	0.53	−16.29	−14.71
MP3/6-311++G(2d,2p)[a]	0.46	0.47	0.93	−15.74	−14.16
MP4D/6-311++G(2d,2p)[a]	0.46	0.49	0.94	−15.62	−14.04
MP4DQ/6-311++G(2d,2p)[a]	0.44	0.47	0.91	−15.52	−13.94
MP4SDQ/6-311++G(2d,2p)[a]	0.44	0.49	0.93	−15.59	−14.01
CCSD/6-311++G(2d,2p)[a]	0.45	0.48	0.93	−15.51	−13.93
CCSD(T)/6-311++G(2d,2p)[a]	0.47	0.55	1.02	−15.70	−14.12

(c) Calculated Counterpoise-Corrected Electronic Interaction Energy ΔE_e(cp), Total Basis Set Superposition Error $BSSE_{total}$, and Zero Point Energy Difference ΔZPE^a in kcal·mol^{-1} for the Cluster $NO^+\cdot(H_2O)_2$ of C_1(b) Symmetry (See Figure 1)

method	BSSE($NO^+\cdot H_2O$)	BSSE(H_2O)	$BSSE_{total}$	ΔE_e(cp)	ΔE_e(cp) + ΔZPE
MP2/6-311++G(2d,p)	0.37	1.36	1.73	−15.09	−12.62
MP2/6-311++G(2d,2p)[a]	0.41	0.95	1.32	−14.70	−12.23
MP2/aug-cc-pVTZ[a]	0.31	0.39	0.70	−15.98	−13.51
MP3/6-311++G(2d,2p)[a]	0.42	0.90	1.32	−13.28	−10.81
MP4D/6-311++G(2d,2p)[a]	0.42	0.92	1.34	−13.49	−11.02
MP4DQ/6-311++G(2d,2p)[a]	0.41	0.88	1.29	−12.58	−10.11
MP4SDQ/6-311++G(2d,2p)[a]	0.41	0.92	1.33	−13.34	−10.87
CCSD/6-311++G(2d,2p)[a]	0.41	0.90	1.31	−13.11	−10.64
CCSD(T)/6-311++G(2d,2p)[a]	0.44	1.00	1.44	−14.51	−12.04

[a] Calculated at the MP2/6-311++G(2p,d) optimized geometry.

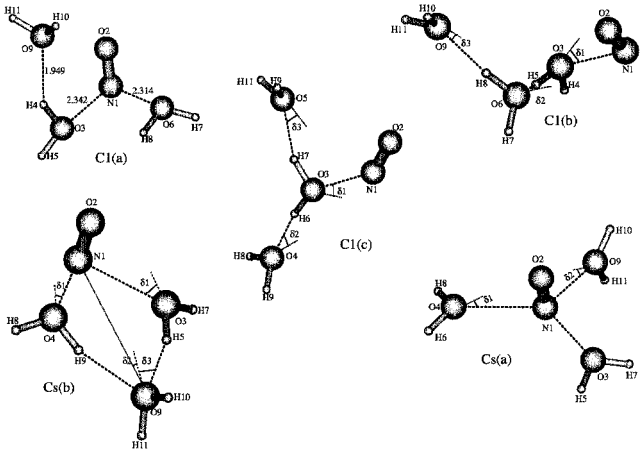

Figure 2. The optimum structures for the isomers of $NO^+\cdot(H_2O)_3$ cluster predicted at MP2/6-311++G(2d,p) level of theory.

vidual stepwise hydration processes in producing the various trihydrate isomers, and are not a direct measure of the relative energies of the various trihydrate isomers. Nevertheless, when the computed relative total electronic energies (Table 4b) and the interaction energies (Table 4c) are compared, it seems that there is a close correspondence between the relative energies of the $NO^+\cdot(H_2O)_3$ isomers and their interaction energies.

The lowest energy structure at the MP2/aug-cc-pVTZ//MP2/6-311++G(2d,p) level (Table 4) is structure C_S(b). It has two water molecules in the first solvation shell, and the third water molecule in the second solvation shell is doubly hydrogen-bonded to the two water molecules of the first solvation shell (see Figure 2). This structure is 0.37 kcal/mol lower in energy than the next isomeric structure, C_S(a), at the MP2/aug-cc-pVTZ level, including corrections for BSSE and ZPE (Table 4c). However, at the MP2/6-311++G(2d,p) level, structure C_S(a) has a more negative interaction energy (CP corrected plus ZPE) than the structure C_S(b). Again, this shows that a large basis set is required in order to obtain reliable relative energies for this type of system.

It is noted that structure C_1(b), which is generated from the isomer C_1(b) in Figure 1 and has the three water molecules in three separate solvation shells, is related to the formation of the $HONO\cdot(H_3O)^+\cdot(H_2O)_2$ adduct (see below). This structure is ca. 3 kcal/mol above the lowest C_S(b) structure at the MP2/aug-cc-pVTZ level (allowing for BSSE and ZPE corrections; see Table 4c).

From the quantum molecular dynamics study of Ye and Cheng,[13] based on a DFT framework, structure C_S(c) was found to be the lowest energy structure. In the present work, it was found to be a saddle point, with one imaginary frequency at the MP2/6-311++G(2d,p) level. The relaxed, minimum-energy structure C_1(c), obtained from the saddle point structure C_S(c), still has one water molecule in the first solvation shell and two water molecules in the second solvation shell. However, the NO^+ fragment has moved toward one of the two water

TABLE 4

(a) Geometries, Electronic Energies, and Standard Entropies for Optimized Structures of $NO^+\cdot(H_2O)_3$ Cluster at MP2/6-311++G(2d,p) Level of Theory; Bond Lengths Are Given in Å, Angles in Degrees

$C_s(b)$[a,b]		C_s(a)[a]		C_1(b)[a]	
$r(N_1-O_2)$	1.0894	$r(N_1-O_2)$	1.0844	$r(N_1-O_2)$	1.0964
$r(N_1-O_3)$	2.3158	$r(N_1-O_3)$	2.4758	$r(O_3-N_1)$	2.0770
$r(H_5-O_9)$	1.9139	$r(O_9-N_1)$	2.4314	$r(O_6-H_5)$	1.6989
$\theta(O_2-N_1-O_3)$	96.9	$\theta(O_3-N_1-O_2)$	90.7	$r(O_9-H_8)$	1.7270
$\theta(O_3-N_1-O_4)$	86.6	$\theta(O_2-N_1-O_9)$	99.9	$\theta(O_3-N_1-O_2)$	104.4
$\theta(O_3-H_5-O_9)$	159.9	$\theta(O_3-N_1-O_9)$	114.1	$\theta(H_5-O_3-N_1)$	99.9
$\omega(O_2-N_1-O_3-H_5)$	111.9	δ_1	18.7	$\theta(O_6-H_5-O_3)$	150.2
$\omega(N_1-O_3-H_5-O_9)$	−22.2	δ_2	10.4	$\theta(O_9-H_8-O_6)$	172.6
$\omega(O_2-N_1-O_3-O_4)$	96.6			$\omega(H_4-O_3-N_1-O_2)$	−169.9
δ_1	30.2			$\omega(H_8-O_6-H_5-O_3)$	96.2
δ_2	1.2			δ_1	54.8
δ_3	40.5			δ_2	38.9
				δ_3	21.8
E_e/Hartree	−358.290756	E_e/Hartree	−358.287109	E_e/Hartree	−358.284203
$S°$/cal·mol^{-1}·K^{-1}	96.5	$S°$/cal·mol^{-1}·K^{-1}	114.6	$S°$/cal·mol^{-1}·K^{-1}	101.6

(b) ab Initio Relative Stabilities in kcal·mol^{-1} and Imaginary Frequencies for the Isomers of $NO^+\cdot(H_2O)_3$ Cluster

	MP2/6-311++G(2d,p)			MP2/aug-cc-pVTZ	
isomer symmetry	E_e	E_e + ZPE[c]	imaginary frequencies	E_e	E_e+ZPE[c]
C_s(b)	0.00	0.00	−	0.00	0.00
C_s(a)	2.29	0.17	−	2.94	0.83
C_1(a)	2.35	1.88	−	2.59	2.11
C_1(c)	2.36	2.06	−	1.49	1.18
C_1(b)	4.11	3.96	−	3.52	3.36
C_s(c)[d]	2.62		−23 (a″)		
C_{3v}[e]	2.37		−53 (a_2)		

(c) Calculated Counterpoise-Corrected Electronic Interaction Energy ΔE_e(cp), Total Basis Set Superposition Error $BSSE_{total}$, and Zero Point Energy Difference ΔZPE[f] in kcal·mol^{-1} for the Isomers of $NO^+\cdot(H_2O)_3$ Cluster (See Figure 2)

isomer symmetry	BSSE($NO^+\cdot(H_2O)_2$)	BSSE(H_2O)	$BSSE_{total}$	ΔE_e(cp)	ΔE_e(cp) + ΔZPE
MP2/6-311++G(2d,p)					
C_1(a)	0.45	1.35	1.80	−13.61	−10.58
C_1(b)	0.33	1.28	1.61	−12.04	−8.79
C_s(a)	0.43	1.08	1.51	−13.97	−12.58
C_s(b)	0.47	1.72	2.19	−15.57	−12.07
MP2/aug-cc-pVTZ					
C_1(b)	0.28	0.35	0.63	−13.28	−10.03
C_s(a)	0.29	0.20	0.49	−14.08	−12.69
C_s(b)	0.41	0.54	0.95	−16.56	−13.06

[a] See Figure 2. [b] The calculated harmonic vibrational frequencies in cm^{-1} (IR intensities in km·mol^{-1}) are: a′: 52(4), 101(4), 201(19), 211(21), 250(119), 262(0), 335(117), 545(143), 723(232), 1632(137), 1673(17), 2083(67), 3664(807), 3783(21), 3868(62), 3887(159); a″: 131(2), 195(1), 208(4), 259(29), 301(39), 417(8), 501(320), 638(60), 1633(48), 3631(69), 3864(333). [c] Calculated at the MP2/6-311++G(2d,p) optimized geometry. [d] In the C_s(c) isomer, the first water molecule constitutes a first solvation shell and binds to the nitrogen end of the NO^+. The second and third water molecules attach to both OHs of the first water molcule completing a second solvation shell. [e] All three water molecules attach to the nitrogen end of NO^+ with C_{3v} symmetry. [f] Calculated at the MP2/6-311++G(2d,p) optimized geometry.

molecules in the second solvation shell, thus distorting the symmetry (C_S) of the saddle point structure. This causes the two water molecules in the second solvation shell to become nonequivalent. The one which is on the side of the O atom of NO^+ (Figure 2), has a longer $O_5\cdots H_7$ hydrogen bond length (1.7097 Å) than that of the other water molecule (1.6405 Å). It also has a bond angle, $O_3H_7\cdots O_5$, of 159.3°, which deviates considerably from linearity (cf. that of the other water molecule, which is 171.5°). All of these observations suggest a possible interaction of NO^+ with one of the two water molecules of the second solvation shell in this isomer. This C_1 structure is 0.26 kcal/mol lower in energy than the corresponding saddle point structure C_S(c) at the MP2/6-311++G(2d,p) level (Table 4b), but is higher than the lowest energy structure C_S(b) by 1.5 kcal/mol at the MP2/aug-cc-pVTZ//MP2/6-311++G(2d,p) level (Table 4b).

Note that structure C_1(a) also has a water molecule in the second solvation shell behaving in a similar way as discussed above for the structure C_1(c), with an even longer $O_9\cdots H_4$ hydrogen bond of 1.949 Å and a more nonlinear $O_9\cdots H_4O_3$ hydrogen bond angle (140.0°; see Figure 2). In addition, structure C_1(a) has an $O_9\cdots O_2$ distance, between the oxygen atoms of the water molecule in the second solvation shell and NO^+, of 2.751 Å. This can be compared with the O···N intermolecular distances of 2.342 and 2.314 Å for the two water molecules in the first solvation shell and NO^+. These geometrical parameters of structure C_1(a) suggest a stronger interaction between the water molecule in the second solvation shell and NO^+ (via the O atom of the latter) than that in structure C_1(c), as discussed above. However, for structure C_1(b), where the three water molecules are in three solvation shells, there is no indication from the geometrical parameters that there is any interaction of the water molecules in the second and/or third solvation shells with NO^+.

$NO^+\cdot(H_2O)_4$. On the basis of the relative energies of the trihydrates structures, eight structures of the tetrahydrate, which were believed to be of low energy, were investigated at the MP2/6-311++G(2d,p) level of optimization (Figure 3). The results are summarized in Table 5. Only one of these structures, C_S(b), is a saddle point, with two imaginary frequencies (Table

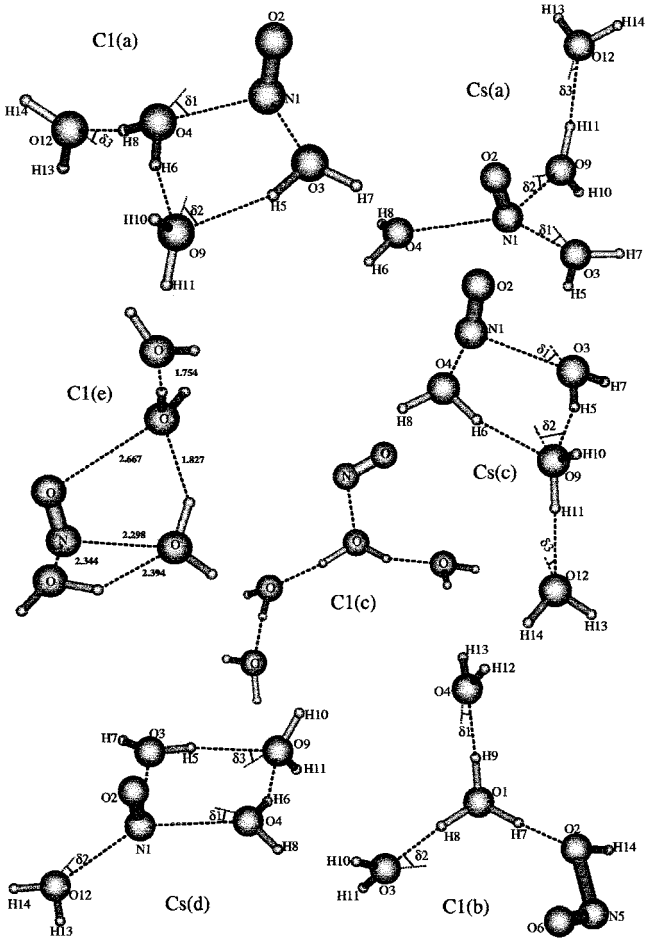

Figure 3. The optimum structures for the isomers of $NO^+\cdot(H_2O)_4$ clusters predicted at MP2/6-311++G(2d,p) level of theory.

5b); this structure is similar to structure C_s(d) in Figure (3) but with the water molecule ($H_{13}O_{12}H_{14}$) rotated 90°. The normal-mode analysis for the vibrations with imaginary frequencies shows that the vibrational motion moves the water molecule ($H_{13}O_{12}H_{14}$) out of the C_S plane. Imposing the symmetry constraint that the water molecule ($H_{13}O_{12}H_{14}$) is at right angles to the mirror plane of C_s symmetry, it optimized to a true minimum; structure C_S(d). Such a rotation of the water molecule in the first solvation shell has lowered the energy by ca. 0.15 kcal/mol, depending on the level of calculation (Table 5b). Structure C_S(d) is the lowest energy minimum obtained in this work for the tetrahydrate complex at the highest level of theory (MP2/aug-cc-pVTZ//MP2/6-311++G(2d,p) plus ZPE and BSSE corrections) considered here. However, the next lowest minimum, structure C_S(c), actually has a lower electronic energy than C_S(d) at the MP2/aug-cc-pVTZ//MP2/6-311++G(2d,p) level of calculation. It is the ZPE and CP correction for BSSE which have reversed the energy ordering of these two minima.

One of the main objectives of this study is to locate the reaction route for nitrous acid and protonated water cluster formation in the stepwise hydration process of NO^+ when the number of water molecules is increased to four, i.e., reaction 2. For this reaction to occur, bond breaking and bond formation have to take place. There are a number of tetrahydrate structures, where such bond breaking and bond formation could take place with minimum changes in the overall geometry of the whole system and these represent favorable conditions for a reaction to proceed. In addition, a transition state (TS) structure may or may not be involved in such a process. If a TS is involved, sufficient energy should be available to overcome the activation energy barrier, in order for the reaction to occur. On the other hand, if there is no TS, the reaction would occur spontaneously, when a water molecule collides with an appropriate trihydrate complex of NO^+, and this would obviously be a favorable route. With these considerations in mind, some of the di-, tri-, and tetrahydrate structures were considered, as mentioned above.

It was found that when a free water molecule was added to the water molecule in the second solvation shell of the trihydrate structure C_1(b) (Figure 2), geometry optimization led to nitrous acid complexed with a protonated water cluster (structure C_1(b) in Figure 3). This suggests that there is a negligible energy barrier for nitrous acid formation, when a free water molecule is added to the *appropriate* trihydrate isomer. Following the geometry changes in the optimization procedure, it appears that a proton transfer from the water molecule of the first solvation shell to the water molecule of the second solvation shell is the initial step of the reaction. Once this proton transfer has taken place, the formation of a protonated water cluster and nitrous acid seems to be straightforward. This route is probably the simplest for HONO and $H^+(H_2O)_3$ formation. Note that Choi et al.[8] proposed a structure for $NO^+\cdot(H_2O)_4$, which has one, one, and two water molecules in the first, second, and third solvation shells, respectively. Fehsenfeld et al.[20] were the first to suggest that this structure might be one of the possible structures which would lead to nitrous acid formation. This suggested structure is actually what we anticipated in the above-mentioned geometry optimization, when one free water molecule was added to the water molecule of the second solvation shell of structure C_1(b) in Figure 2. Of course, without the results of the present calculations, Choi et al.[8] did not realize that their proposed structure for $NO^+\cdot(H_2O)_4$ was not stable, and was not even a stationary point on the energy hypersurface. In addition, Ferguson and co-workers[4,5] could not have foreseen that this structure would lead to $HONO\cdot(H_3O)^+\cdot(H_2O)_2$ formation without a barrier.

Other than structures C_S(d) and C_1(b), structure C_1(e) of the tetrahydrate needs to be discussed. The initial structure of the geometry optimization, which led to the C_1(e) structure, was a free water molecule being added to the terminal water molecule of the trihydrate structure C_1(b) in Figure 2. Thus, it was anticipated that an NO^+ cluster with four water molecules in a chain would result. This chain structure was one of the structures, suggested by Ferguson et al.,[21] which might lead to nitrous acid formation. Geometry optimization, however, led to the unexpected structure C_1(e) shown in Figure 3. The long chain of water molecules has wrapped around the NO^+ moiety, forming a rather complex structure. The second water molecule of the chain moves around to the N atom, becoming the second water molecule of the first solvation shell (with the shortest N···O bond length), while the third water molecule moves around to the O atom of the NO^+ moiety. All four water molecules seem to be linked up by hydrogen-bonding, though the OH···O bond angles are far from linear (except for the terminal one). In structure C_1(e), NO^+ forms a five-membered ring with the second and third water molecules.

General Structural Considerations

Following our previous ab initio study on the protonated water clusters, $H^+\cdot(H_2O)_n$, $n = 1-5$, the structures of cationic-hydrate complexes can be understood in terms of a balance between covalent and ion−dipole hydrogen bonding.[14] It has been shown that the angle between the C_2 axis of a water molecule and the hydrogen bond axis, δ, in a protonated water cluster can be an

TABLE 5

(a) Geometries, Electronic Energies, and Standard Entropies for Optimized Structures of $NO^+ \cdot (H_2O)_4$ Cluster at MP2/6-311++G(2d,p) Level of Theory; Bond Lengths Are Given in Å, Angles in Degrees

$C_s(d)$[a,b]		$C_s(c)$[a]		$C_1(b)$[a]	
$r(N_1-O_2)$	1.0856	$r(N_1-O_2)$	1.0913	$r(O_1-H_7)$	1.0384
$r(N_1-O_3)$	2.4020	$r(N_1-O_3)$	2.2864	$r(O_1-H_9)$	1.0080
$r(N_1-O_{12})$	2.5451	$r(H_5-O_9)$	1.8189	$r(H_7-O_2)$	1.4681
$r(H_5-O_9)$	1.9355	$r(H_{11}-O_{12})$	1.7344	$r(H_8-O_3)$	1.5756
$\theta(O_2-N_1-O_3)$	93.6	$\theta(O_2-N_1-O_3)$	97.5	$r(H_9-O_4)$	1.5653
$\theta(O_2-N_1-O_{12})$	87.6	$\theta(O_3-N_1-O_4)$	87.1	$r(O_2-H_{14})$	0.9739
$\theta(O_3-N_1-O_4)$	85.3	$\theta(O_3-H_5-O_9)$	162.2	$r(O_2-N_5)$	1.7286
$\theta(O_3-H_5-O_9)$	160.5	$\theta(O_9-H_{11}-O_{12})$	176.7	$r(N_5-O_6)$	1.1262
$\theta(O_3-H_5-O_9)$	160.5	$\omega(O_2-N_1-O_3-H_5)$	111.1	$\theta(O_1-H_7-O_2)$	176.5
$\omega(O_2-N_1-O_3-H_5)$	107.8	δ_1	34.6	$\theta(O_1-H_8-O_3)$	175.1
δ_1	26.2	δ_2	40.7	$\theta(O_1-H_9-O_4)$	176.2
δ_2	16.7	δ_3	17.7	$\theta(H_7-O_2-H_{14})$	116.3
δ_3	40.9	δ_4	1.5	$\omega(H_{14}-O_2-N_5-O_6)$	−178.5
δ_4	1.7			δ_1	22.6
				δ_2	26.8
E_e/Hartree	−434.603128	E_e/Hartree	−434.602688	E_e/Hartree	−434.597168
$S°$/cal·mol^{-1}·K^{-1}	122.8	$S°$/cal·mol^{-1}·K^{-1}	114.8	$S°$/cal·mol^{-1}·K^{-1}	116.0

(b) ab Initio Relative Stabilities in kcal·mol^{-1} and Imaginary Frequencies for the Isomers of $NO^+ \cdot (H_2O)_4$ Cluster

	MP2/6-311++G(2d,p)			MP2/aug-cc-pVTZ	
isomer symmetry	E_e	E_e + ZPE[c]	imaginary frequencies	E_e	E_e+ZPE[c]
C_s(d)	0.00	0.00	−	0.00	0.00
C_s(c)	0.28	1.25	−	−0.42	0.55
C_1(a)	0.75	1.53	−	0	0.78
C_s(a)	3.16	2.07	−	3.23	2.13
C_1(c)	3.02	3.79	−	1.55	2.32
C_1(e)	3.03	3.50	−	−	−
C_1(b)	3.74	4.65	−	1.78	2.69
C_s(b)(d)	0.18	-	−32 (a″) −5 (a″)	0.14	−

(c) Calculated Counterpoise-Corrected Electronic Interaction Energy ΔE_e(cp), Total Basis Set Superposition Error $BSSE_{total}$, and Zero Point Energy Difference ΔZPE[e] in kcal·mol^{-1} for the Isomers of $NO^+ \cdot (H_2O)_4$ Cluster (See Figure 3)

isomer symmetry	$BSSE(NO^+ \cdot (H_2O)_3)$	$BSSE(H_2O)$	$BSSE_{total}$	ΔE_e(cp)	ΔE_e(cp) + ΔZPE
MP2/6-311++G(2d,p)					
C_s(d)	0.37	0.96	1.33	−12.65	−11.47
C_s(c)	0.31	1.24	1.55	−12.16	−10.01
C_1(a)	0.34	1.23	1.57	−11.66	−9.70
MP2/aug-cc-pVTZ					
C_s(d)	0.24	0.19	0.43	−12.42	−11.24
C_s(c)	0.26	0.35	0.61	−12.66	−10.51
C_1(a)	0.29	0.34	0.63	−12.21	−10.25

[a] See Figure 3. [b] The calculated harmonic vibrational frequencies in cm^{-1} (IR intensities in km·mol^{-1}) are: a′: 32(3), 66(0), 88(2), 179(2), 192(11), 198(18), 236(58), 244(1), 302(145), 338(348), 517(121), 698(255), 1630(147), 1650(89), 1674(18), 2122(18), 3690(692), 3787(15), 3803(58), 3883(57), 3894(152): a″: 7(0), 78(2), 138(0), 175(0), 205(2), 252(16), 273(17), 330(73), 394(1), 484(374), 617(41), 1637(56), 3664(91), 3880(295), 3910(137). [c] Calculated at the MP2/6-311++G(2d,p) optimized geometry. [d] Similar to C_s(d), but with the fourth water molecule ($H_{13}O_{12}H_{14}$) in plane with N_1O_2 (See Figure 3). [e] Calculated at the MP2/6-311++G(2d,p) optimized geometry.

informative indicator in this respect. For strong ion−dipole interaction, δ is near zero (<5°),[2,14,20] whereas for strong covalent interaction, δ takes larger values (as large as 40°).[2,14] In addition, dispersion effects were found to become more important in the larger clusters (with longer hydrogen bond lengths) and these increase δ. For $NO^+ \cdot (H_2O)_n$ complexes, they do not have a hydrogen bond in the first solvation shell. Nevertheless, the angle between the C_2 axis of the water molecule and the O···N bond, δ, can still be indicative of the type of interaction between the water molecule and NO^+. The computed angles δ are shown in Tables 1a, 2, 4a, and 5a for some relatively low-energy isomers of the mono-, di-, tri-, and tetrahydrates of NO^+, respectively. It can be seen that most of the δ values are significantly larger than zero, suggesting stronger covalent and/or dispersive interactions than ion−dipole interaction. This is the case for all of the NO^+ clusters considered here, for water molecules in the first, second, and third solvation shells. Such behavior is quite different from that in the protonated water clusters.

For both the tri- and tetrahydrates of NO^+ (structure C_S(b) in Figure 2 and Table 4a; structures C_S(c) and C_S(d) in Figure 3 and Table 5a, respectively), it is noted that for the water molecule in the second solvation shell, which is hydrogen-bonded to two water molecules of the first solvation shell, the angle δ with respect to N is near zero. This may suggest some ion−dipole interaction between the water molecule in the second solvation shell and N of NO^+. However, the distance between the O atom of this water molecule and N of NO^+ is rather long (>4 Å). Nevertheless, as has been mentioned above there are some isomeric structures which have a water molecule of the second solvation shell having a possible interaction with the O of NO^+. All of these observations of the isomeric structures of the NO^+ hydrates suggest a much more complicated interaction scheme than that in the protonated water clusters.

From the previous study on protonated water clusters,[14] it was found that, energetically, it was more favorable for the first solvation shell to be completely filled by three water molecules, before starting the second solvation shell. For the NO^+ hydrate clusters, this is not the case. The energy differences between placing water molecules in the different solvation shells are significantly smaller than those for the protonated water clusters. It can been seen that isomeric structures which have the first solvation shell not completely filled by three water molecules actually have lower energy than those with the first solvation shell that is completely filled, for both the tri- and tetrahydrated NO^+ clusters (Figures 2 and 3, and Tables 4b, 4c, 5b, and 5c). In particular, the doubly hydrogen-bonding interaction between the water molecule in the second solvation shell with the two water molecules of the first solvation shell seems to be stronger than the interaction between the third water of the first solvation shell and NO^+, because structure C_s(b) is lower in energy than structure C_s(a) in Figure 2 by 0.37 kcal/mol at the highest level of calculation (see Table 4c). Of course, all of these hydrogen-bonding and water/NO^+ interactions in the NO^+ clusters are interrelated and affect each other. In this connection, one of the most striking and important findings in the present study is the barrierless proton transfer (as discussed above) from the water molecule of the first solvation shell to the water molecule in the second solvation shell on H_2O addition to structure C_1(b) of $NO^+(H_2O)_3$. The formation of the $H^+\cdot(H_2O)_3\cdots$HONO cation, which leads to the formation of nitrous acid, is the result of the dramatic effect of an extra hydrogen bond, caused by the addition of a single water molecule to the right isomeric structure of $NO^+\cdot(H_2O)_3$, C_1(b) in Figure 2.

The thermodynamics of nitrous acid formation as a function of the hydration level n during the stepwise hydration of $NO^+\cdot(H_2O)_n$ complexes will be investigated in part II of this present study.

Vibrational Spectra of $NO^+(H_2O)_n$ Complexes. In the study of $NO^+(H_2O)_{1-3}$ clusters ions by vibrational predissociation spectroscopy,[8] the only photofragment detected on infrared excitation of an $NO^+(H_2O)_n$ ion in the 2700−3800 cm^{-1} region was $NO^+(H_2O)_{n-1}$. Vibrational predissociation spectra recorded by monitoring the signal of the $NO^+(H_2O)_{n-1}$ ion as a function of excitation wavenumber, in the region 2700−3800 cm^{-1}, can be assigned fairly easily to excitation of H_2O asymmetric and symmetric stretching modes. For the $NO^+(H_2O)_{1,2}$ complex ions the low-lying energy minima (the lowest minimum and those within 5 kcal/mol of this structure) are all of the solvated NO^+ type. In the 2000−4000 cm^{-1} region, the vibrational spectra can be classified into three regions. The H_2O asymmetric stretches 3950−3700 cm^{-1}, the H_2O symmetric stretches 3800−3500 cm^{-1}, and the NO stretch 2150−1900 cm^{-1}.

For $NO^+(H_2O)_4$, on excitation in the 3600−3800 cm^{-1} wavenumber range, the branching ratio between production of $NO^+(H_2O)_3 + H_2O$ and $H_3O^+(H_2O)_2$ + HONO was measured in ref 8 as 8:1. Unfortunately, an infrared spectrum was only obtained by monitoring the $NO^+(H_2O)_3$ intensity (and not the $H_3O^+(H_2O)_2$ intensity as well) as a function of laser wavenumber. This predissociation spectrum, recorded in the 2700−3800 cm^{-1} region, could be assigned in terms of the $NO^+(H_2O)_4$ vibrational modes, notably the H_2O asymmetric and symmetric stretching modes, and stretching of the H_2O O−H bonds in the first solvation shell involved in hydrogen bonding.

For $NO^+(H_2O)_5$, on excitation in the 2700−3800 cm^{-1} region, $H_3O^+(H_2O)_3$ was the dominant ion. Monitoring its intensity as a function of laser energy gave a group of bands in the region 3500−3800 cm^{-1} and a broad intense band, not expected for an $NO^+(H_2O)_n$ structure, centered at ≈2800 cm^{-1}. Calculations performed in this work for $H_3O^+(H_2O)_2$HONO and $H_3O^+(H_2O)_3$-HONO show that a strong band is expected in the 2700−2900 cm^{-1} region for an O−H stretching of an H_3O^+ group. The absorptions in the 3500−3800 cm^{-1} region can be assigned to the O−H stretch of HONO group and symmetric and asymmetric stretches of the H_2O groups.

It is clear from these measurements that although the existing infrared spectra can be assigned, it would be useful to extend them to a wider wavenumber range and record the vibrational predissociation spectrum of $NO^+(H_2O)_4$ in the $H^+(H_2O)_3$ channel as well as the $NO^+(H_2O)_3$ channel. Nevertheless, it is clear that for $NO^+(H_2O)_5$, $H_3O^+(H_2O)_{n-2}$ + HONO is the dominant predissociation channel relative to $NO^+(H_2O)_n + H_2O$, whereas for $NO^+(H_2O)_4$ the reverse is true.

Conclusion

In the present work, minimum energy geometries, harmonic vibrational frequencies and stepwise binding energies for the $NO^+\cdot(H_2O)_n$ complexes with $n = 1-4$ were obtained by high-level ab initio calculations. From a systematic investigation of the effects of electron correlation and basis set size for the $NO^+\cdot(H_2O)_n$ complexes with $n = 1-2$, it was found that the MP2/6-311++G(2d,p) level of theory was reliable for the calculation of minimum energy geometries and harmonic vibrational frequencies of the $NO^+\cdot(H_2O)_n$ complexes. It was also found that MP2 theory was adequate for relative energies. However, to keep the basis set superposition error to within 1 kcal/mol in the calculations of binding energies of the $NO^+\cdot(H_2O)_n$ complexes, a basis set of size of at least as large as the aug-cc-pVTZ basis set was needed.

As with the protonated water clusters, $(H_3O)^+(H_2O)_n$,[14] it was found that the first solvation shell of the $NO^+\cdot(H_2O)_n$ hydrates can have a maximum of three water molecules (structure C_S(a) in Figure 2, and structures C_S(a) and C_S(d) in Figure 3). However, the solvation behavior in the $NO^+\cdot(H_2O)_n$ hydrates is quite different from that in the protonated water clusters. In the stepwise hydration processes of the latter, the first solvation shell is filled first before the second solvation shell. In contrast, in the $NO^+\cdot(H_2O)_n$ hydrates, the computed energy differences for structures having a water molecule in the first or the second solvation shell are rather small. For $NO^+\cdot(H_2O)_3$, the lowest energy isomeric structure C_S(b) (Figure 2) has the third water molecule in the second solvation shell rather than filling up the first solvation shell, as in structure C_S(a) in Figure 2. The latter is nearly 3 kcal/mol higher in electronic energy than the former (see Tables 4b and 4c). Similarly, for $NO^+\cdot(H_2O)_4$, the structures C_1(a), C_S(c), and C_S(d) in Figure 3 have computed total energies which are very close to each other (see Tables 5b and 5c). Structures C_1(a) and C_S(c) both have only two water molecules in the first solvation shell. In addition, there are two observations of the solvation behavior of the $NO^+\cdot(H_2O)_n$ hydrates, which are unusual, as compared with the solvation behavior of protonated water clusters. First, although the N end of the NO^+ moiety is the preferred site of hydration, the O end of the NO^+ moiety also interacts with a water molecule in some structures, such as structure C_1(a) in Figure 2, and structure C_1(e) in Figure 3. Second, a number of the isomeric structures have a water molecule in the second solvation shell, which is hydrogen-bonded to two water molecules of the first solvation shell. Summarizing, the solvation behavior of the $NO^+\cdot(H_2O)_n$ hydrates is much more complex than that of the protonated water clusters, resulting in isomeric structures of similar energies.

One of the most important findings in the present investigation is a reaction route for the formation of nitrous acid. The stepwise

hydration processes, which constitute this reaction route, start from $NO^+ \cdot H_2O$, and proceed via structure C_1(b) in Figure 1, and structure C_1(b) in Figure 2. These structures essentially arise from increasing the length of the solvent chain bonded to NO^+. When a fourth water molecule is added to the water molecule of the second solvation shell of the isomeric structure C_1(b) of $NO^+ \cdot (H_2O)_3$ (Figure 2), formation of the nitrous acid protonated water adduct, $HONO \cdot H_3O^+(H_2O)_2$ (structure C_1(b) in Figure 3) occurs spontaneously. This finding provides a plausible reaction mechanism for the recent experimental observations that four water molecules are needed to promote the appearance of protonated water clusters in the hydration process of the NO^+ cation.

Acknowledgment. Financial Support from the EPSRC (U.K.) is gratefully acknowledged.

References and Notes

(1) Hobza, P.; Zahradnik, R. *Intermolecular Complexes: The Role of van der Waals Systems in Physical Chemistry and in Biodisciplines (Studies in Physical and Theoretical Chemistry)*; Elsevier: New York, 1988; Vol. 52.

(2) Kollman, P. A. *Applications of Electronic Structure Theory*; Schaefer, H. F., III, Ed.; Plenum Press: New York, 1978, Vol. 3, p 109.

(3) Wayne, R. P. *Chemistry of Atmospheres*; Oxford University Press: Oxford, 1991.

(4) Fehsenfeld, F. C.; Ferguson, E. E. *J. Geophys. Res.* **1969**, *74*, 2217.

(5) Fehsenfeld, F. C.; Ferguson, E. E. *J. Geophys. Res.* **1969**, *74*, 5743.

(6) Good, A.; Durden, D. A.; Kebarle, P. *J. Chem. Phys.* **1970**, *52*, 222.

(7) French, M. A.; Hills, L. P.; Kebarle, P. *Can. J. Chem.* **1973**, *51*, 456.

(8) Choi, J.-H.; Kuwata, K. T.; Haas, B.-M.; Cao, Y.; Johnson, M. S.; Okumura, M. *J. Chem. Phys.* **1994**, *100*, 7153.

(9) Stace, A. J.; Winkel, J. F.; Martens, R. B. L.; Upham, J. E. *J. Phys. Chem.* **1994,** *98*, 2012.

(10) Angel, L.; Stace, A. J. *J. Chem. Phys.* **1998**, *109*, 1713.

(11) De Petris, G.; Di Marzio, A.; Grandinetti, F. *J. Phys. Chem.* **1991**, *95*, 9782.

(12) Mack, P.; Dyke, J. M.; Wright, T. G. *Chem. Phys.* **1997**, *218*, 243.

(13) Ye, L.; Cheng, H.-P. *J. Chem. Phys.* **1998**, *108*, 2015.

(14) Lee, E. P. F.; Dyke, J. M. *Mol. Phys.* **1991**, *73*, 375.

(15) Paizs, B.; Suhai, S. *J. Comput. Chem.* **1998**, *19*, 575.

(16) Wright, T. G. *J. Chem. Phys.* **1996**, *105*, 7579.

(17) Boys, S. F.; Bernardi, F. *Mol. Phys.* **1970**, *19*, 553.

(18) Frisch, M. J.; Trucks, G. W.; Schlegel, H. B.; Gill, P. M. W.; Johnson, B. G.; Robb, M. A.; Cheeseman, J. R.; Keith, T.; Petersson, G. A.; Montgomery, J. A.; Raghavachari, K.; Al-Laham, M. A.; Zakrzewski, V. G.; Ortiz, J. V.; Foresman, J. B.; Cioslowski, J.; Stefanov, B. B.; Nanayakkara, A.; Challacombe, M.; Peng, C. Y.; Ayala, P. Y.; Chen, W., Wong, M. W.; Andres, J. L.; Replogle; E. S.; Gomperts, R.; Martin, R. L.; Fox, D. J., Binkley, J. S.; Defrees, D. J.; Baker, J.; Stewart, J. P.; Head-Gordon, M.; Gonzalez, C.; Pople, J. A. GAUSSIAN 94, REVISION D.4; Gaussian, Inc.: Pittsburgh, PA, 1995.

(19) Tsuzuki, S.; Uchimaru, T.; Matsumura, K.; Mikami, K.; Tanabe, K. *J. Chem. Phys.* **1999**, *110*, 11906.

(20) Fehsenfeld, F. C.; Mosesman, M.; Ferguson, E. E. *J. Chem. Phys.* **1971**, *55*, 2120.

(21) De Bene, J. E. *J. Phys. Chem.* **1988**, *92*, 2874.